Proc. of SPIE Vol. 1167, Precision Engineering and Optomechanics, ed. D Vukobratovich (Nov 1989) Copyright SPIE

Advanced Flexure Suspension Systems

Russell Rhoads
and
Joseph Tyburski

Lockheed Missles and Space Company, Inc.
Sunnyvale , Ca. 94089-3504

ABSTRACT

An advanced flexural concept has been developed which allows a large angular mirror deflection of +/- 10 degrees in output beam space and position sensing accuracies approaching ± 6 microradians. A resolution of approximately 1 in 100,000 is possible with this design and the test sensors.

Optical systems require precision pointing and positioning mirrors for various applications, i.e. beam alignment and communications. To date, mirrors with two degrees of large angle rotational freedom are of the gimbaled or flexural type. The advanced flexural system decreases overall mirror inertia; this quality also decreases drive motor size and lessens the complexity of the mirror system. Two prominent problems arise in current flexural designs; limited angular displacement and mirror pumping (i.e. mirror motion perpindicular to the face of the mirror). The advanced flexure system addresses these conditions.

Mirror positional accuracy is another key component of active mirror systems. Spherical edge sensing with inductive sensors offers very high resolutions in 2 axes of rotation not possible previously with these devices.

APPROACH

The design of our mirror system was bound by two design goals. The system was to have a field of view of +/- 10 degrees and a pointing accuracy of +/- 6 micro radians in output beam space. In the development of our system two alternatives were considered. They were first a roller bearing type gimbaled suspension and second a flexure mount pivoting type.

The following criteria have been used to narrow the choices to a flexural system. The system had to have the ability to rotate about any two perpendicular axes lying in a plane. There should be no translation along the Z axis.In figure 1, the axes of rotation are x and y.

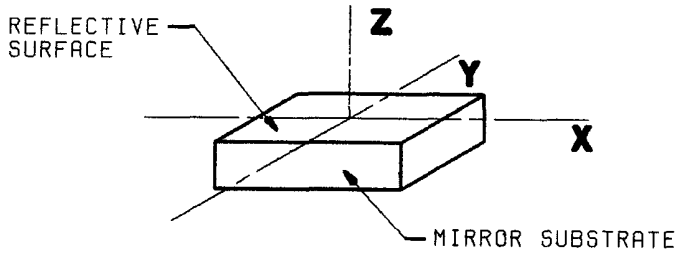

Figure 1

A gimbaled roller bearing suspension system can be designed to be translationally stiff while being torsionally soft. Gimbaled mirrors were rejected because of friction and stiction that prevents the system from obtaining pointing accuracies of +/- 6 microradians in a travel of +/- 10 degrees. For the advanced flexure system, a series of flexure configurations were considered. The selected approach unites a series of wires arranged in a circular pattern and positioned such that they pivoted about a point. This allowed the pointing element to be rotated about any axis in the plane of the surface. The flexure system was oriented such that the center of rotation corresponded to the center of face of the pointing element. The point of rotation can be readily moved to any point desired. In figure 2 the center of rotation is located at the center of gravity. This configuration ensures control loop closure for the system.Two angles of inclination (AOI) were investigated in this study, 22.5 degrees and 45 degrees (see figure 2). A design program taking into account overall mirror system performance was utilized to optimize the flexure system.

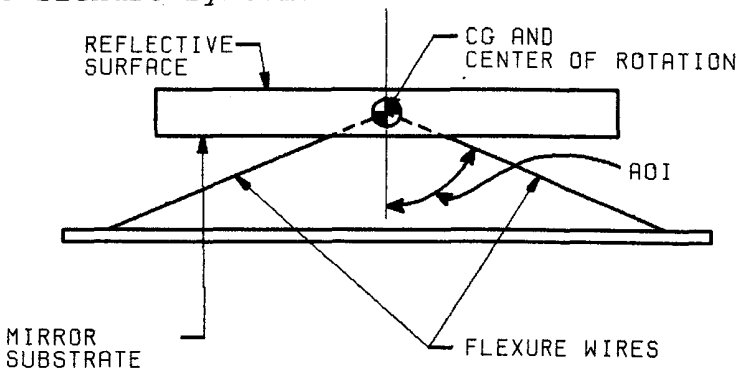

Figure 2

Position knowledge is a requirement in all closed loop control systems. The key consideration in choosing a sensor for our system was, the linear range and resolution of the sensor and physical compatibility with the flexure system. Three types of position sensors were considered; capacitive, inductive and optical encoders. The capacitive position capabilities were limited to less than a degree and did not meet our requirements. The optical encoder was eliminated from consideration because it

was incompatible with the configuration of the flexure. Two inductive types of position sensors were investigated. The first type was the Farrand Controls Inductosyn. The Inductosyn was rejected because, the device itself was incompatible with the flexure configuration. The other inductive device was the Kaman differential measuring system. The Kaman system KD5100 series was selected. This system is essentially a gap measuring device. It uses a pair of matched sensors that read position with respect to a target. The sensors are positioned such that as a target moves away from one sensor through an angle "A" it also moves toward a matched sensor an equivalent amount. A typical application of this system is shown in figure 3. A standard system of four sensors can provide precise rotational measurements about the x and y axes as long as the rotating element remains within the range of the sensors. A typical measuring configuration for this kind of system is shown in figure 4.

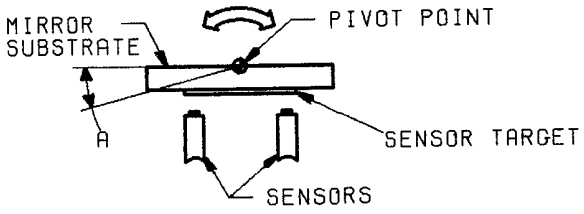

Figure 3.

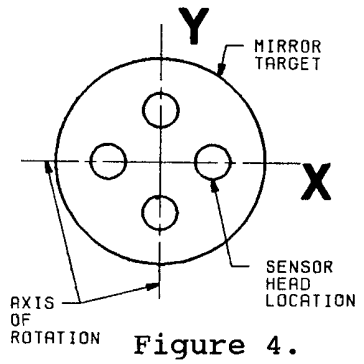

Figure 4.

The most sensitive and wide range sensor that Kaman offers is limited to a null gap of .035 inches. This limited range does not allow the use of the sensors in a conventional manner as shown in figures 3 and 4. Therefore, a different arrangement of these sensors had to be used, the approach was edge sensing.

The initial goal for accuracy was +/- 6 microradians of the output beam, this correlates to +/-3 microradians of pointing element position accuracy. Total range of travel for the element is 10 degrees. This is equivalent to measuring one part in fifty eight thousand (1:58,000).

Range of travel = 10 degrees = 174532 microradians
Positional accuracy = 3 microradians

$$\frac{3}{174532} = \frac{1}{58000}$$

The Kaman sensors have the capability for measurement of approximately 1 in 100,000. The geometry of the present system is set so that measurement accuracy is approximately 2 microradians. In this configuration the target moves across the face of the sensor. Knowing that the measurements are sensitive to the gap

between the target material and the sensor head, our application required the target to sensor gap to be constant as the element rotated. The target was designed to have a spherical face and an edge shown in figure 5.

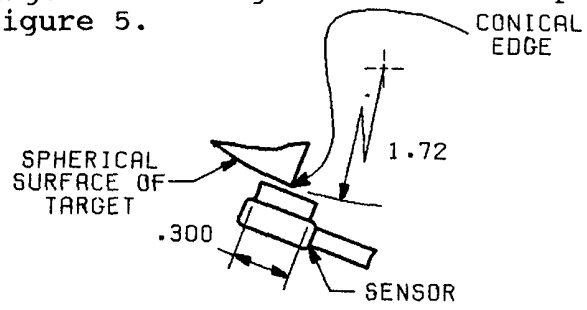

Figure 5.

ANALYSIS AND DESIGN

In order to design our flexure system, it was necessary to understand the application in which the flexure was to be used. For a precision pointing system the necessary factors are:

A) The size and shape of the pointing element

B) The required system bandwidth

C) Characteristics of the pointing element;
   i. Material
   ii. Density
   iii. Modulus of elasticity
   iv. Natural frequency

D) Characteristics of the flexural elements;
   i. Material
   ii. Modulus of elasticity
   iii. Length of flexural elements

E) Characteristics of the actuators;
   i. Approximate size
   ii. Approximate weight
   iii. Approximate center of gravity

Considering the bandwidth of the system as an input, a stiffness ratio, determined by control laws for a stable system, is then calculated for the pointing element. The ratio generally used is for the natural frequency of the element to be ten times the bandwidth of the system. Likewise, for the suspension system, the natural frequency is one-tenth that of the bandwidth of the system.

Next, the inertia of the pointing element is determined by

using the material parameters, geometric envelope and the natural frequency. The actual pointing element natural frequency is desired to be at or above the natural frequency determined by the bandwidth and still retain the external boundary dimensions necessary to meet the requirements of the application. The actuator inertias are then factored in to determine the total mass and area moments of inertia for the pointing element.

Now the initial parameters necessary for the design of the flexure system have been determined. An analysis of the flexural system can be performed, and after making some assumptions the flow chart in figure 6 can be used.

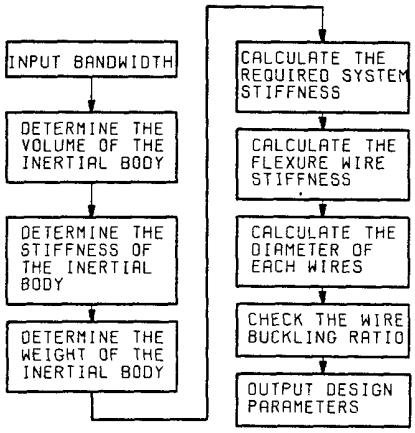

Figure 6.

For a light weighted pointing element it is necessary to add all of the support ribs and structure of the pointing element to obtain the correct mass. The mass of the pointing element is;

$$m_{pes} = \sum_{i=1}^{n} m_i \qquad \text{Eq. 1}$$

The angular acceleration required to attain the system bandwidth is calculated using;

$$\alpha = \omega_{bw}^{2}\, \delta_m \qquad \text{Eq. 2}$$

where, δ_m is the angular displacement and α is the angular acceleration in radians per second of the system oscillating at the bandwidth $F_{b\omega}$ in cycles per second. The bandwidth frequency $\omega_{\beta\omega}$ of the system is in radians per second. Once the acceleration of the system has been established, the torque necessary to meet the system requirements can be calculated from;

$$\text{Torque} = I_0 \alpha \qquad \text{Eq. 3}$$

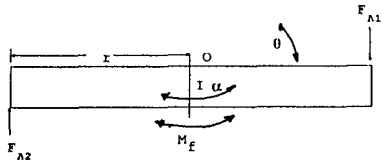

$$\sum_{i=1}^{n} M_o - I_o\alpha = 0 \qquad \text{Eq. 4}$$

$$\sum_{i=1}^{n} M_o - I_o\alpha = 2F_A r\delta - M_F - I_o\alpha = 0 \qquad \text{Eq. 5}$$

ΣM_o is the summation of moments about the point O (the origin) referred to hereafter as the focal point. Summing the moments to zero for the dynamic equilibrium, from the above equation of motion the actuation force F_A, is assumed (for simplification of the problem) to be equally divided between each of the flexural elements.

The natural frequency of the flexural system required, has been determined to be one-tenth the bandwidth of the pointing system. The stiffness of the flexural system can now be determined from the following equation;

$$K_{sys} = \omega^2_{sys} m_{pes} \qquad \text{Eq. 6}$$

where ω_{sys} is the natural frequency of the flexural system and K_{sys} is the stiffness of the flexural system. Once the required K_{sys} has been established the dimensions of the flexural elements can be determined.

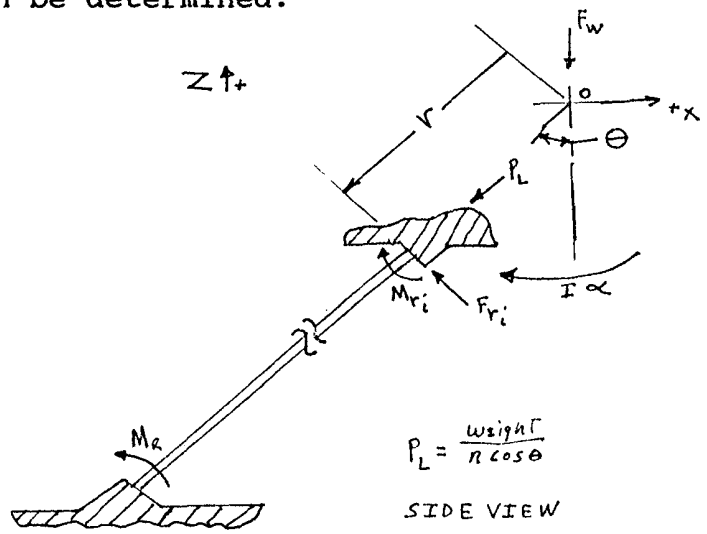

Figure 7.

Looking at figure 7 the direction and magnitude of the forces F caused by the torque are then determined from figure 7, which yields the following equation for each flexural element (wire) including gravity;

$$\sum_{i=1}^{n} F_i = F_{ri}\left(\frac{1}{\cos\theta}\right)\cos\phi_i - \left(\frac{F_w}{n}\right)\left(\frac{1}{\cos\theta}\right) + \left(\frac{M_i}{r_i}\right) \qquad \text{Eq. 7}$$

where F_w is the weight under gravity of the pointing element. F_{ri} is the reaction force at the end of the wire caused by the T_x vector. Θ is the AOI angle between the Z axis and the wires (see figure 2) and is held constant after determination. ϕ_i is the angle between the force F_i and the wire i, it is also equal to 360 divided by the number of wire elements. The number of wires used in the flexure system is n. M_{ri} is the moment created at each end point by the wire being fixed in the rotating member (the pointing element system). Another equation which is used is;

$$\sum_{i=1}^{n} M_o = I\alpha = \sum_{i=1}^{n}(F_{ri}r + M_{ri}) \qquad \text{Eq. 8}$$

in order to solve for the forces F_{ri} and the moments M_{ri}, a matrix of 2n equations would have to be solved simultaneously. Some assumtions have been made to simplify the solution. The following assumptions were made;

A) For small angles the M vector magnitudes are small and therefore neglected.

B) Since all wires have identical dimensions and orientations, the stiffness of all the wires are equal.

C) The flexural elements are located rigidly and perpindicular between two parallel conical surfaces, therefore the deflections are assumed to be the same for each element.

D) Since all other factors are equal the force on each flexural element is assumed to be equal.

E) Using the above assumptions the diameter of the flexural element can be found from the superposition equation for a simply loaded cantilever beam.

Continuing with the above assumptions and the flow chart in figure 6, equation 6 is solved for the required flexural system stiffness and then substituted in equation 10 to determine the stiffness of each flexural element (K_e);

$$K_e = \frac{Ksys}{n} \qquad \text{Eq.9}$$

the stiffness of each flexural element δ_e can also be stated as;

$$K_e = \frac{F_e}{\delta_e} \qquad \text{Eq.10}$$

The deflection of each element δ_e can be found from the superposition equation for the deflection of a simply loaded cantilever beam;

$$\delta_e = \frac{F_e L_e^3}{3E_e I_e} = \frac{F_e}{K_e} \qquad \text{Eq.11}$$

Solving the deflection equation 12 for the element stiffness and noticing that the flexural element force F_e drops out, K_e then becomes;

$$Ke = \frac{3EI_e}{l^3} \qquad \text{Eq.12}$$

The only unknown in equation 13 is the diameter of the flexural element in the area moment of inertia I_e, which has been assumed to be the inertia of cylindrical element;

$$I_e = \frac{\pi d^4}{64} \qquad \text{Eq.13}$$

The flexural element diameter can now be solved for with the following equation:

$$d_w = \sqrt[4]{\frac{64K_e l^3}{3\pi E}} \qquad \text{Eq.14}$$

where E is the modulus of elasticity of the wires and l is the assumed length in the input conditions.From the initial input conditions a check of the buckling conditions can be made. Buckling is a function of the ratio between the length of the wire and its diameter. The recommended maximum buckling ratio is 195:1 (l :d). Having checked the buckling ratio and insuring that it is less than 195:1 the flexure calculations are complete. The force required for the actuators to maintain the bandwidth could be calculated from equation 5 to complete the system design.

The design of the sensing system entailed purchasing a standard sensor device from Kaman. Utilizing edge sensing technology the Kaman sensing system could be used to obtain the required resolution. The target is placed on the backside of the pointing element. It has a spherical face, with a conical lip cut at the bottom portion of the face. This conical lip is cut such that the conical face will come to a point at the focal point. The conical face also forms a 90 degree angle with the surface and is seen as an edge at the face of the Kaman sensor.

The sensing activity functions as follows, a reference voltage is set to zero at a zero degree angular deflection. The target is designed such that as the edge of the target moves to a

position where less material is exposed to one sensor, the opposing edge moves to cover a greater portion of the opposite sensor in the matched pair. The two sensing elements act as differential voltage devices and yield a net voltage output. The output voltage is correlated to position and used as an analog input to the control electronics (see figure 5).

TESTING

Preliminary testing of the pointing system has been done. Some of the tests are rough order of magnitude measurements to demonstrate the validity of this concept and will be repeated later with higher accuracy measuring devices.

The following tests were performed to determine if this flexure concept would be feasible. First a model was constructed that consisted of six flexural elements and had an approximate system rotational natural frequency of .01 Hz with a load of 10 pounds on top. The model worked as expected and indicated that the flexure concept had merit.

A second flexure was made with an upper and lower plate of aluminum and music wires for the flexural elements. An epoxy bond was used as a joint connection. Testing showed the epoxy bond sheared and the joints failed at a deflection of 10 degrees. Test specimens showed that for model purposes (ease of assembly and disassembly was required) soldering was a viable solution. Solder joints were used with the further flexural studies and no further joint failures occured when proper solder application was done.

The first test of the flexure was to find out if the flexure moved axially along the Z axis when the system was deflected in the X and Y axes. In order to perform a rough order of magnitude check, a dial indicator was placed at the focal point and the Z axis deflection was too small to be measured, even at X and Y deflections of 10 degrees. The dial indicator used had a 0.001 inch capability. In order to determine the relationship between the axial stiffness and the radial stiffness, the vertical displacement was measured based on the following relationship;

$$K_{axial} = \frac{\pi D^2 E}{L} \qquad \text{Eq.15}$$

$$K_{radial} = \frac{3\pi E D^4}{64 L^3} \qquad \text{Eq.16}$$

$$\frac{K_{axial}}{K_{radial}} = \frac{3 D^2}{64 L^2} \qquad \text{Eq.17}$$

Using the average displacement of two dial indicators located at opposite corners below the pointing element, weights were placed on the focal point and displacements measured. Knowing the vertical force and the corresponding vertical displacement the stiffness could be dtermined. From the data for this test the stiffness ratio was determined to be approximately 5000 : 1.

The system was tested for linearity of angular torque using a precision target and laser beam alignment system. Figures 8 and 9 show two views of the test setup. First a precision target was prepared, the target was then located vertically such that when a laser beam was calibrated to a reference point and then displaced, forming a triangle. The sine of the angle formed by the laser beam, deflected by a mirror on the flexure system, yields the vertical distance from the reference point. The cosine of the angle is the distance from the mirror face to the reference point. Using the arctangent the angle of interest is found.

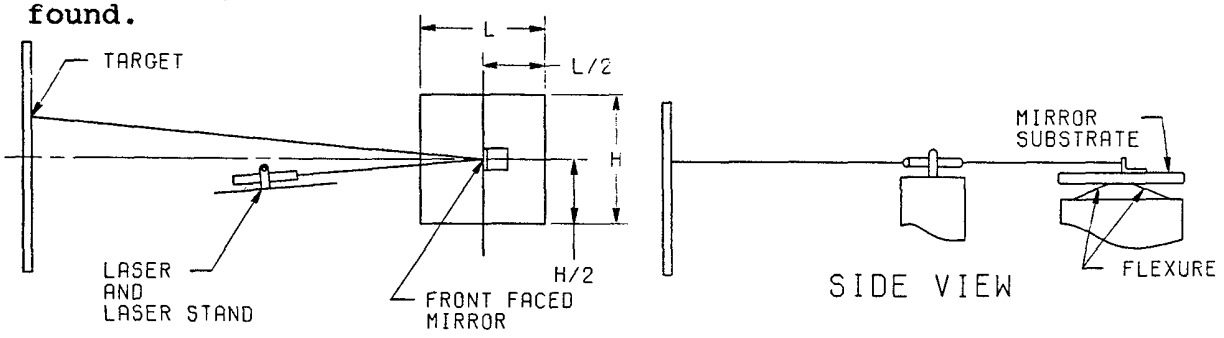

Figure 8

Figure 9

The angular stiffness for the flexural system comes from the equation;

$$T = Fd = K\theta \qquad \text{Eq.18}$$

where is the angular deflection, d is the distance from the center of rotation at which the force is applied and F is the force perpindicular to the axis of rotation, also K is the angular stiffness;

$$K = \frac{Fd}{\theta} \qquad \text{Eq.19}$$

once the angular stiffness was found, a curve for the torque vs. angular deflection was derived. Data from lab setup on the 45 degree angle flexure, was used as a basis for the torque vs. angular deflection. The torque proved to be almost linear, an intercept indicates that minor hysterisis is present. Preliminary analysis indicates that voids exist in the solder joints and when

put under stresses will tend to collapse over time. As discussed advanced hardware will have a more reliable joint and will be tested to see that the hysterisis is eliminated or predictable enough to be compensated for in a control system as is done with some current flexure systems.

The angular stiffness of the flexure (for the various configurations) tested to be between 6 and 45 in-oz/degree of deflection measured at the pointing element. This is a low torque resistance for the inertial decrease benefit gained.

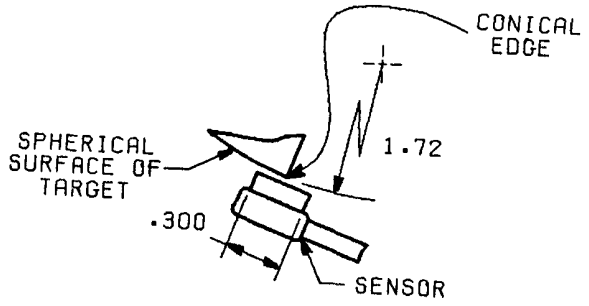

Figure 10

Testing of the sensors indicated the linear portion of the sensor head is limited to .24 inches. Experimental data, taken with a spherical target evalution fixture, indicated that measurements were linear from +8.5 volts to -8.5 volts. This corresponds to +/- .12 inches on the face of the sensor when the measured edge was centered on the sensor head. Voltage output was measured to the nearest .1 of a miilivolt.

.0001 V	least step
17 V	full range
174.5xE-3	full mirror rotation

(.0001/17) x 174.5xE-3 = 1.0 microradian

This results in a potential positional accuracy of 1 microradian, well within our design goal of 3 microradians.

CONCLUSION

The advanced flexure system concept looks promising. The flexure system was tested to +/- 10 degrees of output beam space, the results yielded a linear torsional spring constant. The spring was torsionally soft and axially stiff. Developement of the flexure analysis program will aid in future flexure based systems in a variety of applications, some of which could only be done by gimbals prior.

The new application of the Kaman KD5100 series differential measuring system in sensing a sphereical edge target has also produced promising results. It appears that a measurement accuracy of +/- 3 microradians is obtainable over the large angular travel.